

# Transgenic zebrafish model of the C43G human insulin gene mutation

Stefani C Eames<sup>1,2†</sup>, Mary D Kinkel<sup>1‡</sup>, Sindhu Rajan<sup>3</sup>, Victoria E Prince<sup>1,2</sup>, Louis H Philipson<sup>2,3\*</sup>

## ABSTRACT

**Aims/Introduction:** The human insulin gene/preproinsulin protein mutation C43G disrupts disulfide bond formation and causes diabetes in humans. Previous *in vitro* studies showed that these mutant proteins are retained in the endoplasmic reticulum (ER), are not secreted and are associated with decreased secretion of wild-type insulin. The current study extends this work to an *in vivo* zebrafish model. We hypothesized that C43G-green fluorescent protein (GFP) would be retained in the ER, disrupt  $\beta$ -cell function and lead to impaired glucose homeostasis.

**Materials and Methods:** Islets from adult transgenic zebrafish expressing GFP-tagged human proinsulin mutant C43G (C43G-GFP) or wild-type human proinsulin (Cpep-GFP) were analyzed histologically across a range of ages. Blood glucose concentration was determined under fasting conditions and in response to glucose injection. Insulin secretion was assessed by measuring circulating GFP and endogenous C-peptide levels after glucose injection.

**Results:** The majority of  $\beta$ -cells expressing C43G proinsulin showed excessive accumulation of C43G-GFP in the ER. Western blotting showed that C43G-GFP was present only as proinsulin, indicating defective processing. GFP was poorly secreted in C43G mutants compared with controls. Despite these defects, blood glucose homeostasis was normal. Mutant fish maintained  $\beta$ -cell mass well into maturity and secreted endogenous C-peptide.

**Conclusions:** In this model, the C43G proinsulin mutation does not impair glucose homeostasis or cause significant loss of  $\beta$ -cell mass. This model might be useful for identifying potential therapeutic targets for proper trafficking of intracellular insulin or for maintenance of  $\beta$ -cell mass in early-stage diabetic patients. (*J Diabetes Invest* doi: 10.1111/jdi.12015, 2013)

**KEY WORDS:** Islets of langerhans/pathology, Misfolded proinsulin, Neonatal diabetes

## INTRODUCTION

Specific heterozygous mutations in the insulin gene cause diabetes in humans and mice<sup>1–9</sup>. Insulin gene mutations are a common cause of permanent neonatal diabetes<sup>10</sup>, and have also been shown to cause MODY10<sup>2,5,6,9,11</sup> and type 1b diabetes<sup>6</sup>. These mutations act in a dominant manner, causing insulin-dependent diabetes even in the presence of one normal insulin allele in humans, and three normal insulin alleles in mice. Several of these mutations lie in critical conserved residues that are involved in the formation of disulfide bonds required for proper folding of the proinsulin protein. Experiments using mouse models<sup>1,3,12</sup> and cell lines<sup>4,9,13,14</sup> have shown that these misfolded proteins accumulate in the endoplasmic reticulum (ER), leading to reduced insulin secretion,  $\beta$ -cell death, and eventually diabetes. One such insulin gene mutation is human

proinsulin (hproinsulin) C43G, which causes neonatal diabetes in humans, but has yet to be characterized *in vivo* in a model system.

A critical step in insulin biosynthesis is the post-translational formation, within the ER, of three intramolecular disulfide bonds (A6-A11, A7-B7 and B19-A20) that function to stabilize the properly folded proinsulin protein. Proinsulin is then trafficked to secretory granules, where proteolytic cleavage results in the conversion of proinsulin to native insulin and the C-peptide. The C43G mutation (amino acid position 43 in the human preproinsulin protein) disrupts the normal formation of the B19-A20 disulfide bond. This mutation has a similar effect to that of the Akita mouse (*Ins2<sup>WT/C96Y</sup>*), which prohibits the formation of the A7-B7 disulfide bond<sup>1</sup>. In a previous study, we expressed 10 different hproinsulin mutant proteins, including C43G, in transiently transfected MIN6 mouse insulinoma cells, and characterized their behavior and effect on secretory function<sup>13</sup>. Several of the mutant proteins, including C43G, were retained in the ER to a significant degree, likely as a consequence of their misfolding. These mutant proteins failed to be processed from the proinsulin form or trafficked to secretory granules, and therefore were not secreted in response to glucose stimulation. Although expression of C43G mutant proinsulin

<sup>1</sup>Department of Organismal Biology and Anatomy, <sup>2</sup>Committee on Molecular Metabolism and Nutrition, and <sup>3</sup>Department of Medicine, University of Chicago, Chicago, Illinois, USA

\*Corresponding author. Louis H Philipson Tel: +1-773-702-9180 Fax: +1-773-834-0851 E-mail address: lphilipson@uchicago.edu

†Present address: Diabetes Center, University of California-San Francisco, San Francisco, CA, USA

‡Present address: Sanford Research, Sioux Falls, SD, USA

Received 12 June 2012; revised 5 August 2012; accepted 22 August 2012

did not inhibit trafficking of co-expressed wild-type proinsulin to secretory granules, release of wild-type insulin was attenuated, suggesting impaired secretory function<sup>13</sup>. Additional studies of the C43G mutation showed similar results, and studies on a variety of human insulin mutations that cause misfolding showed that multiple such mutations are associated with impaired secretory function<sup>4,14,15</sup>. Indeed, human patients with neonatal diabetes generally have undetectable levels of circulating C-peptide and require insulin therapy<sup>16</sup>.

In the present study, we took advantage of the zebrafish model to study the long-term effects of C43G mutant hproinsulin on  $\beta$ -cell function *in vivo*. We generated transgenic zebrafish expressing either normal hproinsulin or the C43G hproinsulin mutant. Each transgene included the green fluorescent protein (GFP) coding region inserted into the C-peptide of proinsulin, allowing us to visualize expression of the transgene *in vivo*, and to use circulating GFP as an indicator of human insulin release<sup>13</sup>.

## MATERIALS AND METHODS

### Generation of Transgenic Lines

The *Tg(-1.0ins:Hsa.INS-GFP)<sup>ch101</sup>* line (*Tg[Cpep-GFP]*) was made using a 995-bp fragment of the zebrafish preproinsulin gene promoter upstream of Cpep-GFP within the T2KXIGAIN Tol2 transposon vector<sup>17</sup>. The Cpep-GFP fragment includes human preproinsulin with the GFP coding sequence within the C-peptide, between proline 72 and glycine 73, as previously reported<sup>13</sup>. The Cpep-GFP element was amplified by polymerase chain reaction (PCR) with primers to introduce NcoI and ClaI restriction endonuclease recognition sites (forward [NcoI]: 5'-cccatgccATGGCCCTGTGGATGCGCCT-3', reverse [ClaI]: 5'-ggatcgatCTAGTTGCAGTAGTTCTCCAGCTG-3'). The Cpep-GFP segment replaced the eGFP coding sequence in the *ins:eGFP/pT2KXIGAIN* plasmid<sup>18</sup>, to generate *ins:Hsa.INS-GFP/pT2KXIGAIN*. For the *Tg(-1.0ins:Hsa.INS<sup>C43G</sup>-GFP)<sup>ch102</sup>* line (*Tg[C43G-GFP]*), the C43G mutation was introduced into *ins:Hsa.INS-GFP/pT2KXIGAIN* by PCR (QuikChange Site-Directed Mutagenesis Kit; Stratagene, La Jolla, CA, USA) and its presence was confirmed by sequencing. Transgenic zebrafish were generated as described<sup>19</sup>. Briefly, construct DNA was co-injected with transposase messenger ribonucleic acid into fertilized eggs from AB wild-type fish. Positive embryos were identified by GFP fluorescence at 2–3 days post-fertilization (dpf). The Tol2 transposon system creates single copy insertions<sup>20</sup>. As we used F2 progeny from in-crossed F1 fish in all experiments, each fish analyzed expressed two copies of the transgene.

### Zebrafish Lines and Maintenance

Zebrafish were raised and cared for using standard procedures<sup>21</sup>. Experimental procedures were approved by the University of Chicago Institutional Animal Care and Use Committee. Additional zebrafish lines were used: wild-type (AB), *Tg(-4.0ins:GFP)<sup>z5</sup>* (referred to as *Tg[ins:GFP]*)<sup>22</sup>, *Tg(h2afv:GFP)* (referred to as *Tg[H2A.GFP]*)<sup>23</sup>. The *Tg(ins:GFP)* line reports GFP

expression in  $\beta$ -cells. The *Tg(H2A.GFP)* line expresses a fusion of GFP to histone variant H2A.F/Z.

### Immunofluorescent Antibody Staining

Embryos were fixed for 1–2 days in 4% paraformaldehyde (PFA) at 4°C. Whole-mount immunofluorescent staining was carried out following standard procedures. Gut organs dissected en bloc were fixed in 4% PFA for at least 12 h at room temperature. Paraffin sections (5  $\mu$ m) were stained using standard immunofluorescent procedures. Primary antibodies included polyclonal rabbit anti-GFP (Molecular Probes, Eugene, OR, USA; 1:2000), monoclonal mouse anti-GFP (Clontech, Mountain View, CA, USA; 1:2000), polyclonal guinea pig anti-insulin (DAKO, Carpinteria, CA, USA; 1:200), monoclonal mouse anti-glucagon (Sigma, St. Louis, MO, USA; 1:200), monoclonal mouse anti-KDEL (Abcam, Cambridge, MA, USA; 1:200), monoclonal rabbit anti-BiP (Cell Signaling, Danvers, MA, USA; 1:200) and monospecific rabbit anti-zebrafish C-peptide (Pacific Immunology, Ramona, CA, USA; 1:500). The zebrafish C-peptide antibody was produced using a synthetic peptide corresponding to PKSAQETEVADFAFKD. Primary antibodies were detected with AlexaFluor-conjugated secondary antibodies (1:2000). Samples were mounted with ProLong Gold Antifade reagent containing 4',6-diamidino-2-phenylindole nuclear stain (Molecular Probes). Staining with anti-KDEL and anti-immunoglobulin binding protein (BiP) required antigen retrieval (boiling in sodium citrate buffer, pH 6). Embryos and sections were imaged by confocal microscopy (Leica TCS SP2 or SP5; Leica, Heidelberg, Germany). Images were processed using NIH ImageJ software (National Institutes of Health, Bethesda, MD, USA).

### Western Blotting

Principal islets were dissected and pooled from three adult fish, placed into radio-immunoprecipitation assay lysis buffer (Santa Cruz Biotechnology, Santa Cruz, CA, USA) containing Complete Protease Inhibitor Cocktail tablets (Roche, Indianapolis, IN, USA), sonicated and heated at 80°C for 10 min before adding sample loading buffer and loading onto a 12% tris-glycine gel (Invitrogen, Carlsbad, CA, USA). Proteins were transferred onto a nitrocellulose membrane and probed with rabbit anti-GFP (Invitrogen; 1:500), followed by horseradish peroxidase-conjugated anti-rabbit IgG (Jackson ImmunoResearch, West Grove, PA, USA; 1:3000) and detected using SuperSignal West Femto Chemiluminescent Substrate (Thermo Scientific, Rockford, IL, USA). Blots were imaged using the ChemiDoc XRS gel documentation system (Bio-Rad, Hercules, CA, USA).

### Glucose Challenge

Glucose challenge was carried out as previously described<sup>24</sup>. Briefly, after a 3-day fast, adult fish were injected intraperitoneally with 0.75 mg glucose per gram bodyweight. Whole blood was collected using heparinized microhematocrit tubes, and

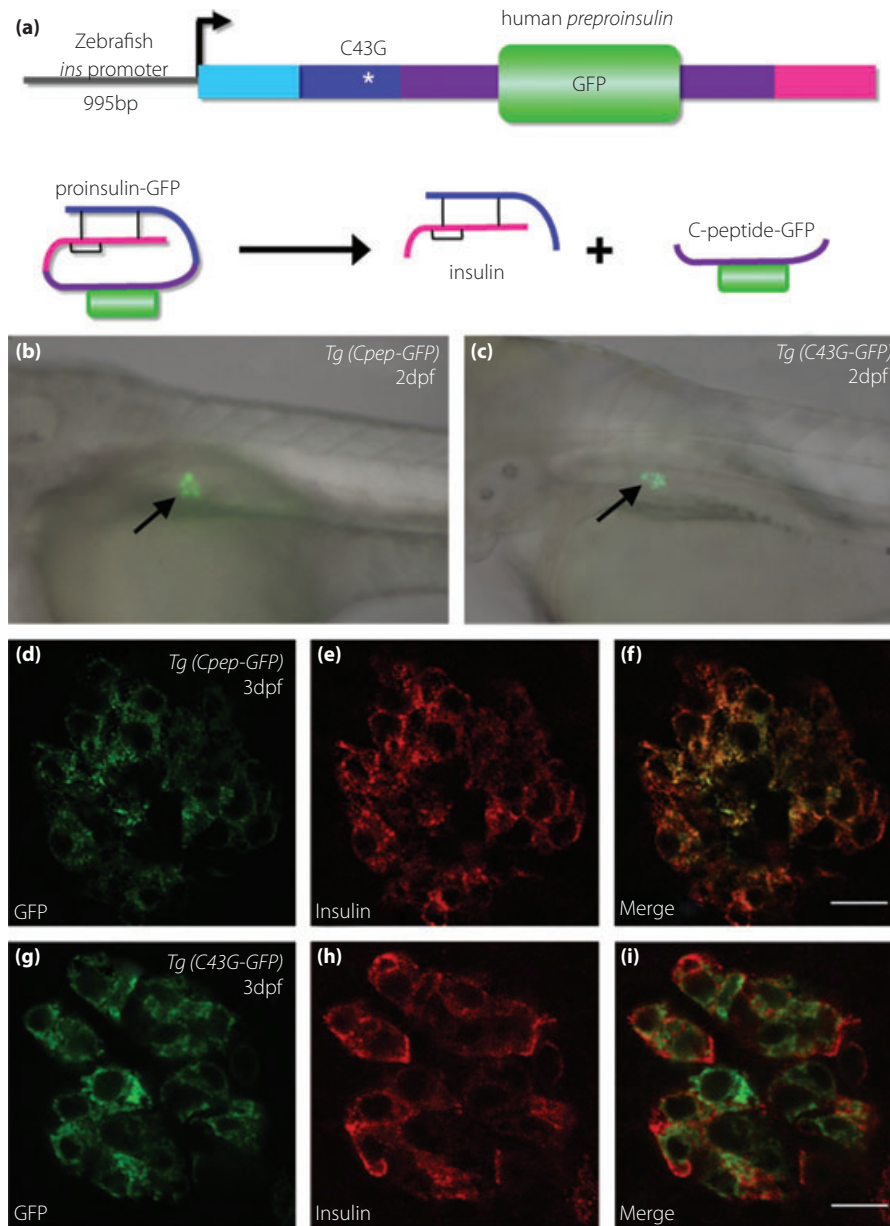


**Figure 1** |  $\beta$ -Cell specific expression of green fluorescent protein (GFP)-tagged human proinsulin in transgenic zebrafish. (a) Schematic diagram of transgene construct used to drive expression of Cpep-GFP or C43G-GFP in zebrafish  $\beta$ -cells. Construct encodes human preproinsulin with GFP (green) within the C-peptide (purple). Location of the C43G mutation in the B-chain (dark blue) is shown (\*). Diagram depicts processing of folded proinsulin-GFP. Three disulfide bonds (black lines) stabilize the conformation of the A-chain (pink) and B-chain (blue). Proteolytic cleavage of proinsulin-GFP liberates C-peptide-GFP from insulin. (b,c) Fluorescent images of live *Tg(Cpep-GFP)* and *Tg(C43G-GFP)* 2-dpf larvae, showing expression of each transgene (visible by GFP fluorescence) within the pancreatic islet (arrows). Lateral views, anterior to the left. (d–i) Confocal images of 3 dpf larvae after staining for GFP (green) and insulin (red), showing  $\beta$ -cell specific expression of each transgene. The insulin antibody recognizes zebrafish and wild-type human insulin, but not the mutant form. *Tg(Cpep-GFP)*,  $n = 7$ ; *Tg(C43G-GFP)*,  $n = 10$ . Bars, 10  $\mu\text{m}$ .

glucose concentration was measured using a FreeStyle Lite glucometer (Abbott, Alameda, CA, USA).

#### GFP and C-Peptide Secretion Assays

Adult fish were fasted for 3 days and a subset were injected with glucose, as aforementioned. Plasma was separated from

whole blood pooled from three to four fish, as described<sup>24</sup>. Circulating GFP was measured by GFP enzyme-linked immunosorbent assay (ELISA; Cell Biolabs, San Diego, CA, USA). Circulating endogenous C-peptide was measured by ELISA utilizing a custom rabbit anti-zebrafish C-peptide antibody (Pacific Immunology).

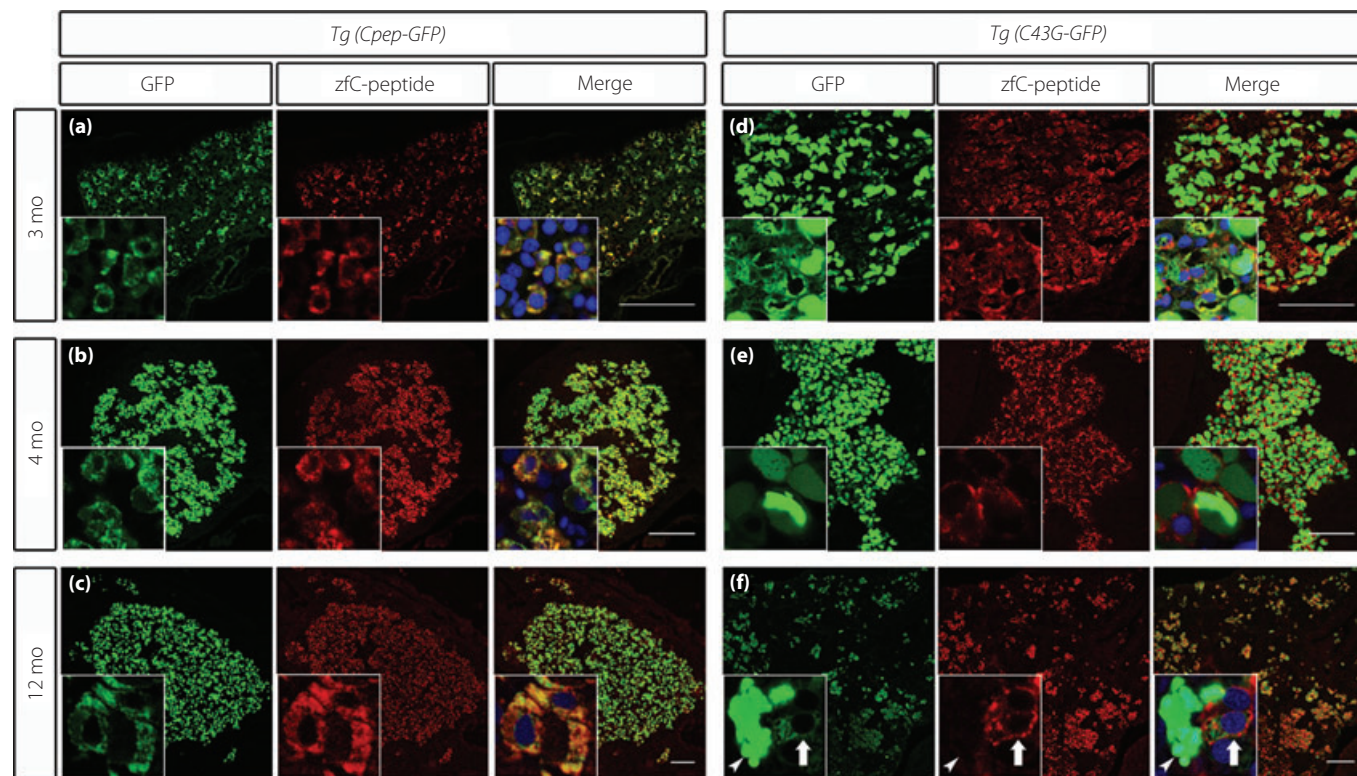


**Figure 2** | Localization of zebrafish C-peptide and human proinsulin in adult islets. Confocal images of staining for green fluorescent protein (GFP; green) and zebrafish C-peptide (red). (a–c) Cpep-GFP expression in adults. GFP is restricted to  $\beta$ -cells and is colocalized with endogenous C-peptide in secretory granules (see insets for high magnification views). (d–f) C43G-GFP expression in adults. C43G-GFP expression is specific to  $\beta$ -cells. Accumulation of C43G-GFP results in irregular cell morphology (see insets for high magnification views). For (f), note that  $\beta$ -cells are significantly scattered. Arrowhead in (f) indicates an enlarged amorphous cell with dramatic GFP accumulation; arrow indicates a cell with less accumulation and a more regular morphology. Note: saturation of pixels in (d–f) is due to the massive accumulation of GFP in a subset of cells. The laser was set at the lowest power that allowed visualization of the subpopulation of cells with low accumulation of GFP. Nuclei were stained with 4',6'-diamidino-2-phenylindole (blue). *Tg(Cpep-GFP)*,  $n = 2$ –5; *Tg(C43G-GFP)*,  $n = 1$ –3. Bars, 100  $\mu$ m.

### Cryo-Electron Microscopy

Principal islets were harvested from 3- to 4-month-old fish, and cryoprotected with Liebovitz L-15 medium (Invitrogen) plus dextran, mannitol and ficol. Islets were immediately frozen in a high-pressure freezer (HPM 010 RMC; BAL-TEC, Balzers, Liechtenstein), and freeze substituted and prepared for imaging as previously reported<sup>25</sup>.

## RESULTS

### Wild-Type and Mutant C43G Human Proinsulin are Expressed Specifically in $\beta$ -Cells of Transgenic Zebrafish

For *in vivo* analysis of hproinsulin, we generated stable transgenic zebrafish lines with  $\beta$ -cell-specific expression of wild-type or mutant C43G hproinsulin driven by the zebrafish preproinsulin gene promoter (*Tg(Cpep-GFP)* and *Tg(C43G-GFP)*, respectively). Both transgenes encode human preproinsulin with GFP inserted within the C-peptide (Figure 1a). GFP does not interfere with hproinsulin folding or processing, and thus provides a convenient means of analyzing hproinsulin subcellular localization and protein processing<sup>13,26,27</sup>. As C-peptide and insulin are secreted

together in equimolar ratios<sup>28</sup>, plasma GFP concentration can be used as a read-out of human insulin release in these fish.

Islet-specific transgene expression was visible by fluorescent imaging in live embryos by 2 dpf (Figure 1b,c). *Tg(Cpep-GFP)* and *Tg(C43G-GFP)* zebrafish developed normally and reproduced as adults, indicating that transgene expression did not impair development. Immunofluorescent staining for GFP and insulin in 3-dpf larvae confirmed  $\beta$ -cell specific expression of each transgene, and that the transgene was expressed in all  $\beta$ -cells (Figure 1d–i). Furthermore, we detected colocalization of Cpep-GFP with endogenous zebrafish insulin in a primarily punctate cytoplasmic pattern consistent with insulin secretory granules (Figure 1d–f). By contrast, C43G-GFP occupied a compartment largely distinct from endogenous insulin, suggesting a trafficking defect of mutant hproinsulin (Figure 1g–i).

To test whether this apparent trafficking defect was a developmental defect associated only with larval maturation, we analyzed transgene expression in adults. Immunofluorescent staining for GFP and zebrafish C-peptide at 3, 4 and 12 months confirmed that the larval staining patterns persisted

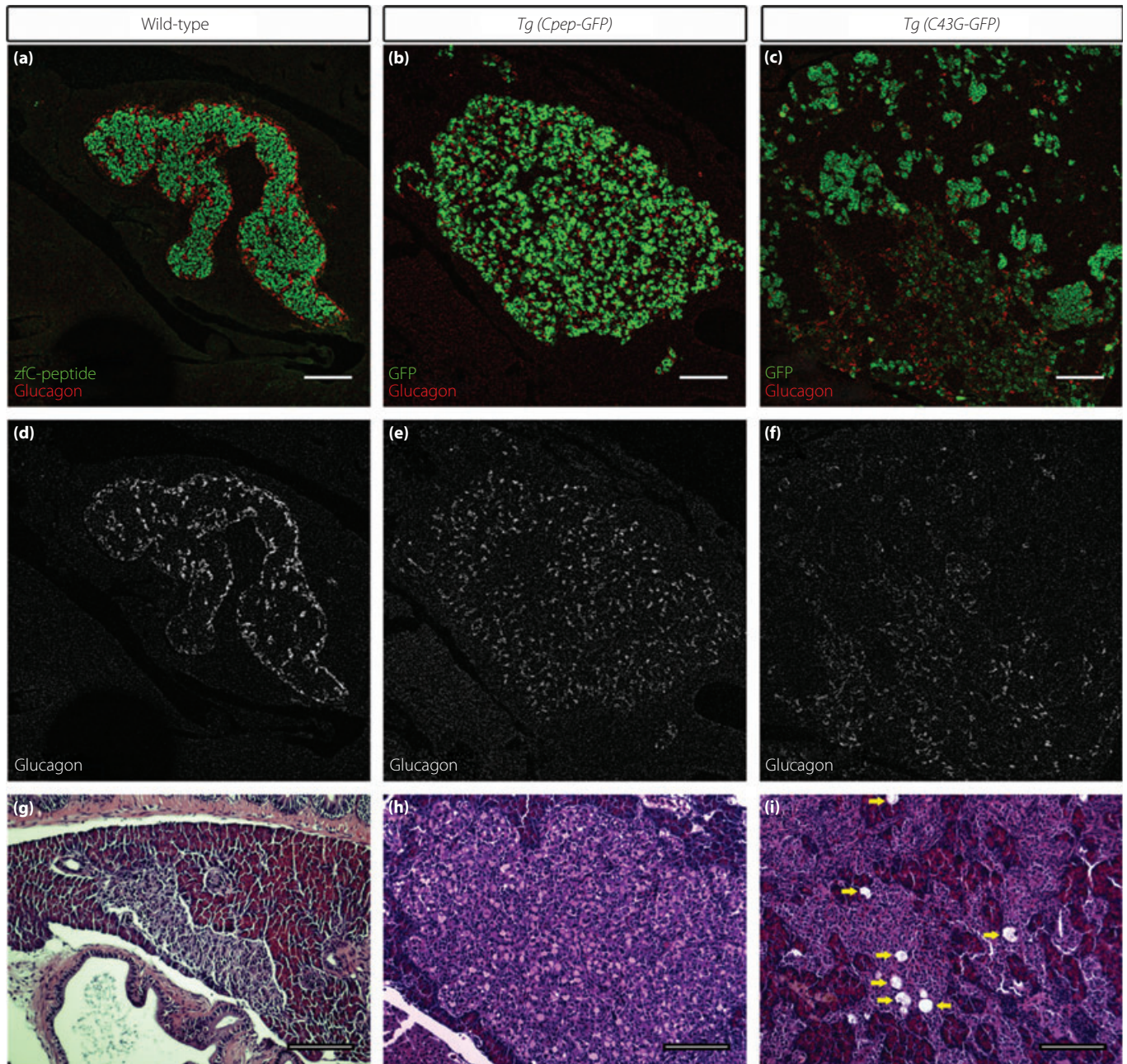


**Figure 3** | Islet architecture is abnormal in *Tg(Cpep-GFP)* and *Tg(C43G-GFP)* adults. (a–c) Staining for glucagon (red) and either zebrafish C-peptide (green in [a]) in wild-type islets or green fluorescent protein (GFP; green in [b,c]) in transgenic islets. (d–f) Red channel alone, showing glucagon expression in  $\alpha$ -cells. AB,  $n = 2$ ; *Tg(Cpep-GFP)*,  $n = 2$ ; *Tg(C43G-GFP)*,  $n = 2$ . (g–i) Hematoxylin–eosin staining of adjacent sections. Arrows in (i) indicate lacunae. All panels: 12 months. Bars, 100  $\mu$ m.

with age (Figure 2). In *Tg(Cpep-GFP)* fish, at each age, Cpep-GFP and endogenous C-peptide were colocalized in a predominantly punctate pattern characteristic of proper packaging of wild-type hproinsulin into secretory granules (Figure 2a–c). By contrast, in adult *Tg(C43G-GFP)* fish, islets contained dysmorphic  $\beta$ -cells that stained intensely for GFP, indicating excessive accumulation of mutant hproinsulin by 3 months (Figure 2d–f). At each age, islets contained morpho-

logically distinct subpopulations of C43G-GFP-expressing cells. One subpopulation showed a staining pattern similar to  $\beta$ -cells seen in larval fish and had modest accumulation of GFP (Figure 2f inset, arrow; compare with Figure 1g–i), whereas a second subpopulation showed dysmorphology and massive accumulation of GFP (Figure 2f inset, arrowhead).

We also observed alterations in islet architecture in both transgenic lines. Wild-type islets were characterized by a mantle

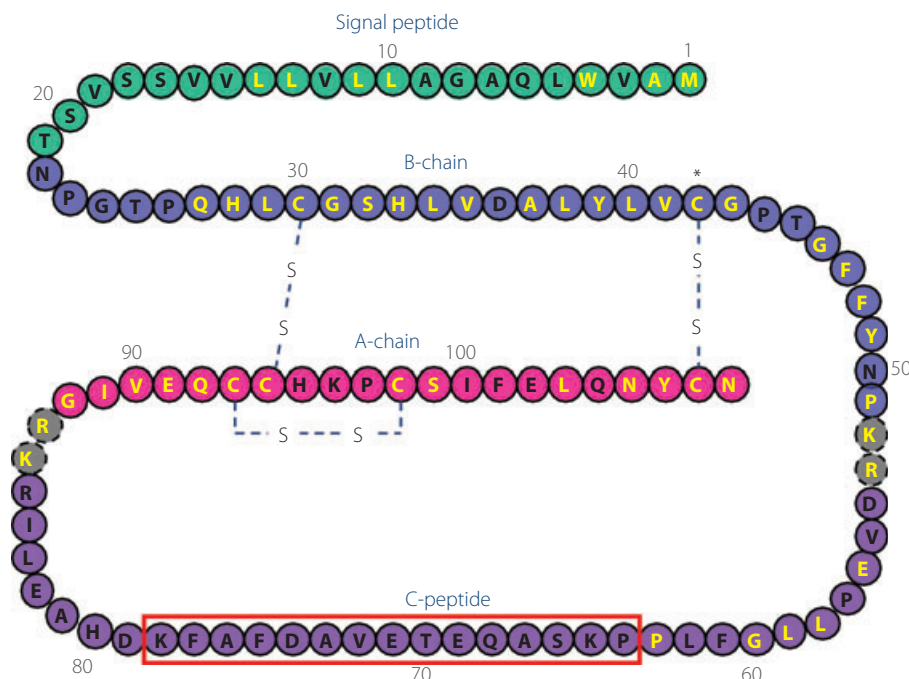


**Figure 4** | Conservation of residues in human and zebrafish preproinsulin. Schematic diagram of zebrafish preproinsulin protein, with amino acids conserved with human preproinsulin protein in yellow. Residues are color-coded: signal peptide (green), B-chain (blue), C-peptide (purple), A-chain (pink), cleavage sites (gray). Disulfide bonds are indicated as (-S-S-). Location of the human C43G mutation is indicated with an asterisk (amino acid position 42 in the zebrafish preproinsulin protein). The red box indicates the peptide recognized by the anti-zebrafish C-peptide antibody. Note the absence of shared residues between the human and zebrafish proteins in this region.

of glucagon-expressing  $\alpha$ -cells surrounding a core of tightly-associated  $\beta$ -cells (Figure 3a). In transgenics, there was no detectable mantle of  $\alpha$ -cells (Figure 3b–c). Instead,  $\alpha$ -cells were intermingled with  $\beta$ -cells throughout the islet. In *Tg(C43G-GFP)* islets, architecture was further disrupted by invasion of the islet by exocrine tissue (Figure 3c,i). Histological analysis showed that *Tg(C43G-GFP)* islets contained numerous lacunae, suggesting cell loss<sup>29</sup> (Figure 3g–i). Although lacunae were detected in some *Tg(Cpep-GFP)* islets (1/5 at 4 months, 4/8 at 12 months), they were more prevalent in *Tg(C43G-GFP)* islets (3/4 at 4 months, 8/8 at 12 months). These changes in islet architecture are reminiscent of the rearrangements observed in multiple zebrafish models of  $\beta$ -cell regeneration<sup>30,31</sup>. We hypothesize that in the *Tg(C43G-GFP)* fish, there is increased  $\beta$ -cell turnover, and that this might be a key mechanism allowing the maintenance of  $\beta$ -cell mass throughout life.

#### Mutant Proinsulin Fails to be Processed or Secreted

Our histological analyses showed that wild-type hproinsulin colocalized with zebrafish insulin in secretory granules, whereas mutant hproinsulin was absent from secretory granules. Human and zebrafish preproinsulin protein sequences show conservation of residues in regions critical to folding and processing (Figure 4). We therefore hypothesized that in our transgenic lines, wild-type hproinsulin was properly folded and processed

by endogenous hormone convertases, whereas mutant hproinsulin was not. Western blot analysis using an anti-GFP antibody showed that in adult *Tg(Cpep-GFP)* islets, the prominent band represented C-peptide-GFP, as expected (Figure 5a). Thus, GFP-tagged wild-type hproinsulin was correctly processed in zebrafish  $\beta$ -cells. In contrast, analysis of adult *Tg(C43G-GFP)* islets showed the absence of the free C-peptide-GFP band and the presence of a prominent band at ~37 kDa, which corresponded to proinsulin-GFP, showing that mutant hproinsulin did not undergo proteolytic processing. As proinsulin processing occurs in secretory granules, this is consistent with our immunohistological observations showing failure of mutant proinsulin to colocalize with endogenous zebrafish insulin in secretory granules.

To test whether C43G-GFP hproinsulin fails to be trafficked to secretory granules, we analyzed circulating GFP levels in both transgenic lines and in a negative control line, *Tg(H2A.GFP)*, in which GFP secretion into the blood was not expected. In plasma from *Tg(Cpep-GFP)* control fish, circulating GFP was readily detected (Figure 5b). Conversely, plasma GFP levels in *Tg(C43G-GFP)* fish were not significantly different from those in the negative controls. These findings suggest that in

*Tg(Cpep-GFP)* control fish, trafficking of hproinsulin to secretory granules allows its release into the circulation, whereas in

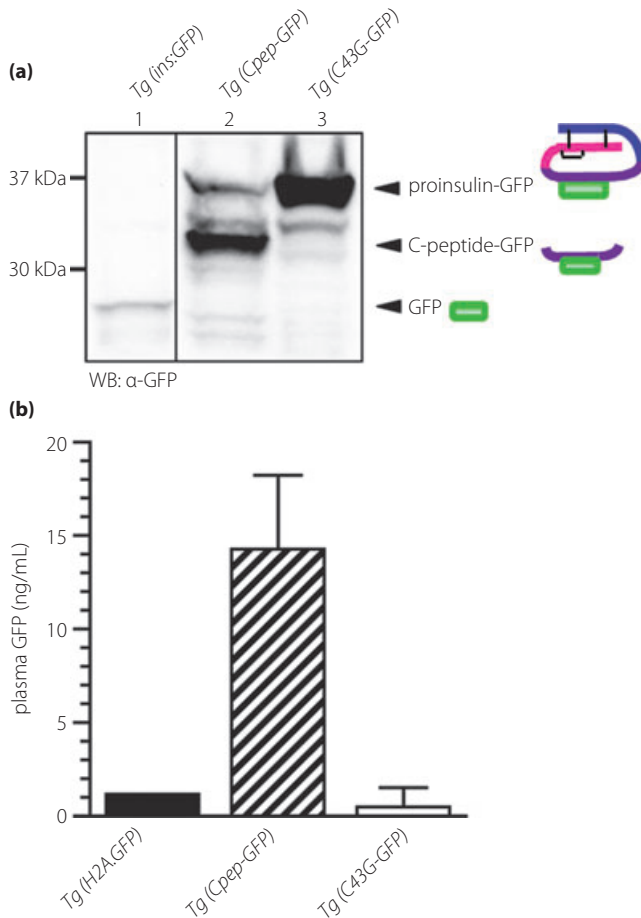


**Figure 5** | C43G-green fluorescent protein (GFP) is not processed from proinsulin or secreted. (a) Lysate of principal islets from *Tg(Ins-GFP)*, *Tg(Cpep-GFP)* and *Tg(C43G-GFP)* adults were analyzed by western blotting with anti-GFP antibody to detect processing of proinsulin-GFP to insulin and C-peptide-GFP. Lane 1 shows free GFP. Lane 2 shows a prominent band for processed C-peptide-GFP and fainter bands running more slowly that indicate partial processing of the Cpep-GFP protein. Lane 3 shows a high molecular weight band for unprocessed proinsulin-GFP, and smaller bands corresponding to partial processing products. The black line between lanes 1 and 2 indicates reassembly of non-contiguous gel lanes. The blot shown is representative of two independent experiments. (b) Thirty minutes after intraperitoneal glucose injection, blood was collected and pooled from three to four adult fish, and plasma was analyzed by GFP enzyme-linked immunosorbent assay. Plasma from *Tg(H2A-GFP)* fish was used as a negative control, as GFP was not expected to be secreted into the blood. Data are mean  $\pm$  standard error of the mean,  $n = 1-3$  independent experiments.

*Tg(C43G-GFP)* mutant fish, retention of misfolded hproinsulin in the ER might prevent its secretion.

#### Mutant Proinsulin Accumulates in the ER

To test whether mutant hproinsulin was retained in the ER, we immunofluorescently labeled KDEL, the ER retention sequence,

and the ER-resident chaperone BiP (Figure 6). Neither marker showed intense staining in wild-type  $\beta$ -cells (Figure 6a,b). We found that in *Tg(Cpep-GFP)* islets, most  $\beta$ -cells strongly expressed both KDEL and BiP. A subpopulation of  $\beta$ -cells was characterized by an enlarged ER (Figure 6c,d), which likely reflects the increased processing demands required by expression of the human insulin transgene. Consistent with our analysis showing localization of human wild-type insulin to secretory granules (Figure 2), we did not detect significant colocalization of Cpep-GFP with the ER. Ultrastructural analysis showed the distended ER as a compartment with relatively low electron-density occupying a significant portion of the cytoplasm (Figure 6h), which was not observed in wild-type  $\beta$ -cells (Figure 6g). Other organelles including mitochondria, Golgi apparatus and nuclei appeared normal (Figure 6h, and data not shown).

Similar analyses on islets from *Tg(C43G-GFP)* fish showed colocalization of mutant hproinsulin with the ER proteins, KDEL and BiP (Figure 6e,f). As with *Tg(Cpep-GFP)*  $\beta$ -cells, the ER was often distended, occupying much of the cytoplasm. Intriguingly, we found that  $\beta$ -cells showed a range of severity of ER distention, such that some cells had little-to-no distention (Figure 6e, arrow) and others were more severely affected (Figure 6e, arrowhead). Ultrastructural analysis confirmed that the varying ER morphologies manifested as a range in size and differences in electron density (Figure 6i,j, and data not shown). ER compartment size varied from cell to cell, from those that showed smaller ER compartments sized similarly to mitochondria, to cells in which the ER were larger and occupied the majority of the cytoplasm.

#### Adult Zebrafish Maintain Euglycemia Despite Expression of the Human Proinsulin C43G Mutant Protein

Expression of insulin gene mutant C43G causes diabetes in humans despite the presence of one normal insulin allele. Our previous *in vitro* studies suggest that impaired trafficking and secretion of C43G mutant hproinsulin in mammalian cells is associated with decreased secretion of wild-type insulin and might contribute to  $\beta$ -cell dysfunction<sup>13</sup>. Similarly, studies using the Akita mouse model (*Ins2<sup>WT/C96Y</sup>*) have shown that impaired trafficking of the mutant protein results in ER stress,  $\beta$ -cell death and the inability to maintain blood glucose homeostasis<sup>12,32,33</sup>. We therefore tested the hypotheses that adult *Tg(C43G-GFP)* fish are hyperglycemic as a consequence of impaired  $\beta$ -cell function, and that this condition worsens with time. To evaluate glucose homeostasis, we measured blood glucose concentration under fasting conditions across an age range. We did not detect hyperglycemia in age-matched wild-type, *Tg(Cpep-GFP)* or *Tg(C43G-GFP)* fish (Figure 7a). At 8 and 12 months, *Tg(C43G-GFP)* mean blood glucose values were somewhat elevated relative to age-matched controls, but the concentrations were not indicative of hyperglycemia. Analysis of blood glucose concentration within groups through time showed no statistically significant relationship with age, and comparisons of the slopes of the trendlines showed no signifi-

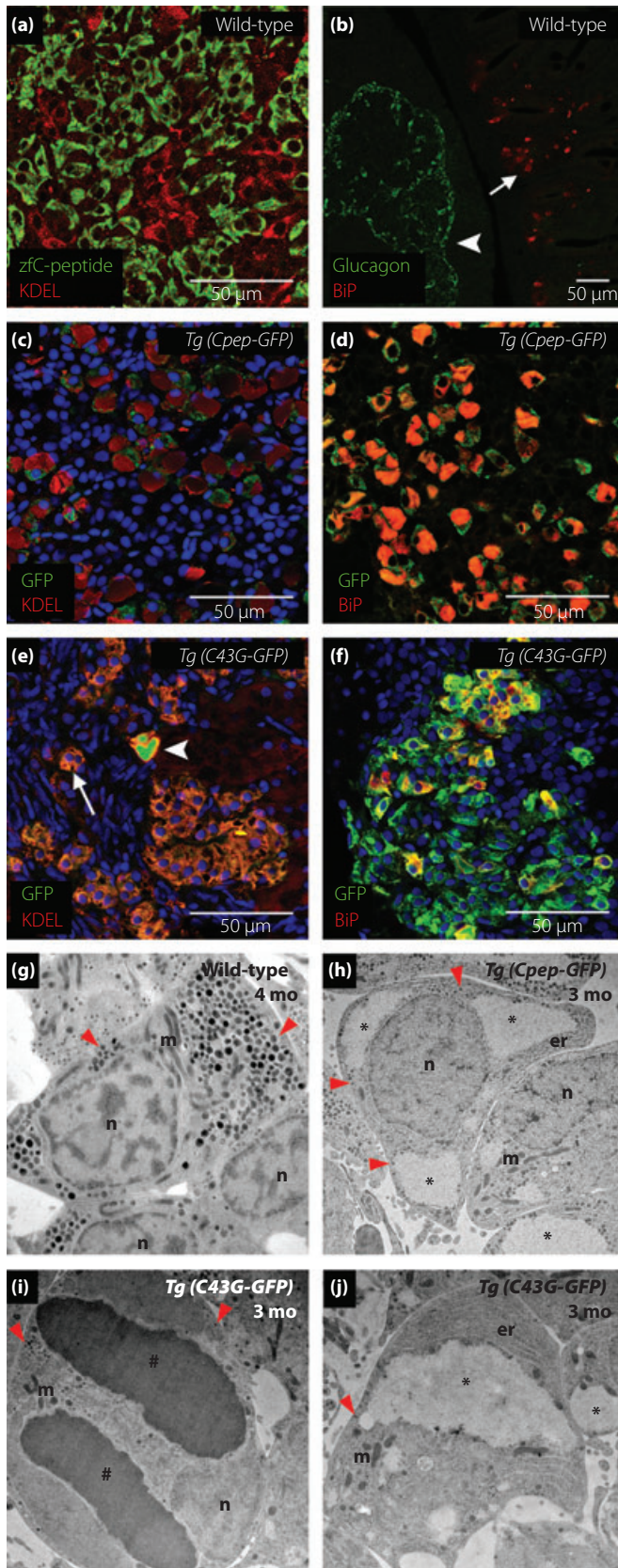


**Figure 6** | C43G-green fluorescent protein (GFP) is retained in the endoplasmic reticulum (ER). (a) Staining for zebrafish C-peptide (green) and KDEL (red) in wild-type islet shows low labeling for KDEL in  $\beta$ -cells ( $n = 4$ ). (b) Staining for glucagon (green) and immunoglobulin binding protein (BiP; red) in wild-type islets ( $n = 2$ ). BiP expression is not detected in the islet (arrowhead), but does stain the adjacent intestine (arrow).  $\beta$ -Cells lie inside the mantle of glucagon-positive  $\alpha$ -cells. Magnification is lower to reveal positive intestinal BiP staining. (c) KDEL (red) staining is expanded within many  $\beta$ -cells in *Tg(Cpep-GFP)*, whereas GFP (green) staining is largely confined to secretory granules ( $n = 3$ ). (d) BiP (red) and GFP (green) staining in *Tg(Cpep-GFP)* shows a similar pattern as seen in (c) ( $n = 2$ ). (e) KDEL (red) staining highlights variable ER morphology in *Tg(C43G-GFP)* islets ( $n = 4$ ). Arrow indicates expanded ER network with GFP accumulation. Arrowhead indicates an example of a  $\beta$ -cell with a highly expanded ER and extensive GFP localized to the ER lumen. (f) BiP (red) and GFP (green) staining in *Tg(C43G-GFP)* shows colocalization ( $n = 3$ ). BiP staining is increased in subpopulations of  $\beta$ -cells. (a–f) 12 months. Bars, 50  $\mu$ m. (c,e,f) Nuclei were stained with 4',6-diamidino-2-phenylindole (blue). (g–j) Electron micrographs of  $\beta$ -cells in wild-type, *Tg(Cpep-GFP)* and *Tg(C43G-GFP)*. Arrowheads, secretory granules; n, nucleus; m, mitochondria; er, normal ER; \*, distended ER with low electron density; #, distended ER with high electron density. All electron micrographs were taken at the same magnification.

cant difference between groups (Figure 7b). We concluded that blood sugar homeostasis was maintained in *Tg(C43G-GFP)* fish under fasting conditions.

Next, we asked whether *Tg(C43G-GFP)* fish would be able to efficiently regulate blood glucose in response to an intraperitoneal glucose challenge. A total of 30 min after glucose injection, we found that blood glucose concentrations were not significantly higher than wild-type or *Tg(Cpep-GFP)* fish across the same age groups tested in the fasting study (Figure 7c). Thus, for zebrafish, unlike humans, expression of hproinsulin mutant C43G was not associated with hyperglycemia, suggesting that these fish were able to secrete endogenous insulin. To test this, we measured circulating levels of endogenous zebrafish C-peptide by custom ELISA using an anti-zebrafish C-peptide antibody specifically designed to not recognize human proinsulin or C-peptide (Figure 4, red box). We found comparable levels of circulating zebrafish C-peptide in age-matched wild-type, *Tg(Cpep-GFP)* and *Tg(C43G-GFP)* fish, indicating that expression of C43G-GFP did not impair secretion of endogenous insulin (Figure 7d).

## DISCUSSION

The C43G insulin mutation is a dominant heterozygous mutation that causes permanent neonatal diabetes in humans. This mutation has been predicted to disrupt  $\beta$ -cell function as a result of aberrant accumulation of misfolded proinsulin in the ER, attenuation of insulin secretion and loss of  $\beta$ -cell mass through apoptosis<sup>2,13,14</sup>. To test this hypothesis, we developed an *in vivo* model using transgenic zebrafish expressing the C43G human proinsulin (hproinsulin) mutant protein. We

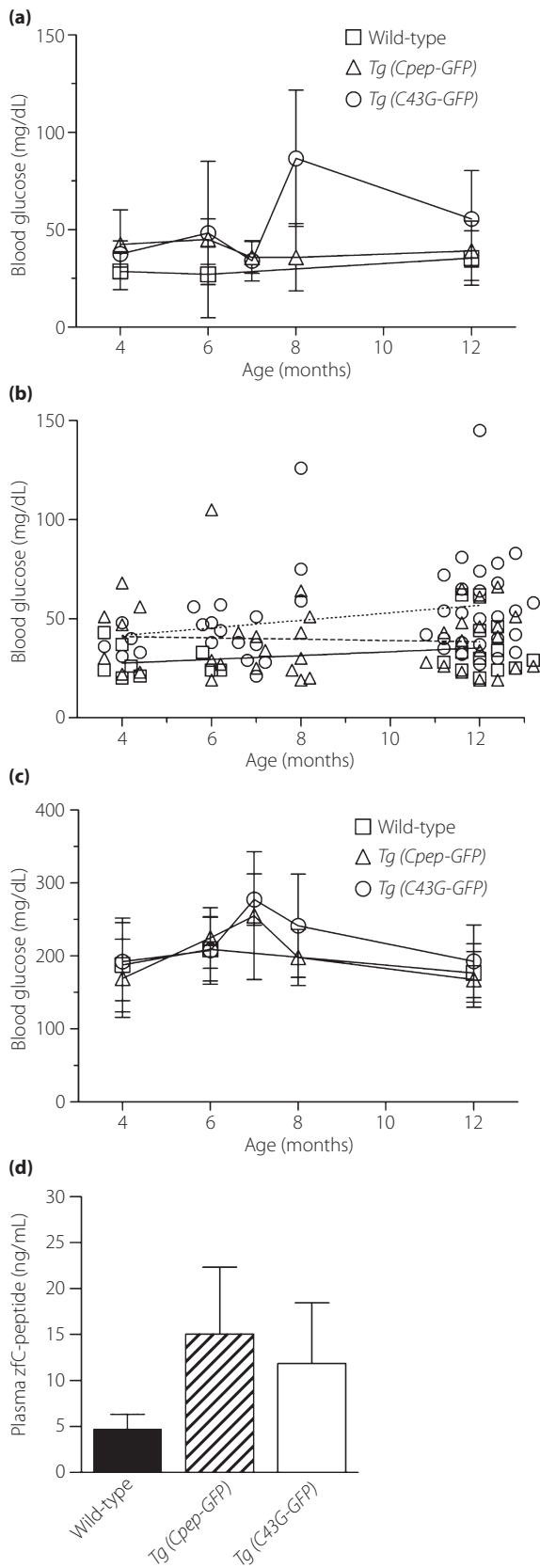


**Figure 7** | Adult mutant fish are euglycemic. (a) Blood glucose concentration after a 3-day fast (wild-type: 4 months,  $n = 6$ ; 6 months,  $n = 3$ ; 12 months,  $n = 13$ . *Tg(Cpep-GFP)*: 4 months,  $n = 7$ ; 6 months,  $n = 4$ ; 7 months,  $n = 4$ ; 8 months,  $n = 7$ ; 12 months,  $n = 18$ . *Tg(C43G-GFP)*: 4 months,  $n = 5$ ; 6 months,  $n = 6$ ; 7 months,  $n = 6$ ; 8 months,  $n = 3$ ; 12 months,  $n = 26$ ). (b) Scatter plot for individual data points shown in (a). Linear trendlines for wild-type = solid line, *Tg(Cpep-GFP)* = dashed line, *Tg(C43G-GFP)* = dotted line. Linear regression analysis showed no statistically significant relationship with age within groups (*Tg(C43G-GFP)*,  $r^2 = 0.061$ ,  $P = 0.0989$ ; *Tg(Cpep-GFP)*,  $r^2 = 0.003$ ,  $P = 0.7280$ ; AB,  $r^2 = 0.088$ ,  $P = 0.1795$ ), and no statistically significant difference between groups in the slopes of the trendlines ( $P = 0.2742$ ). (c) Blood glucose concentration 30 min after intraperitoneal glucose injection (wild-type: 4 months,  $n = 7$ ; 6 months,  $n = 3$ ; 12 months,  $n = 12$ . *Tg(Cpep-GFP)*: 4 months,  $n = 8$ ; 6 months,  $n = 4$ ; 7 months,  $n = 4$ ; 8 months,  $n = 7$ ; 12 months,  $n = 18$ . *Tg(C43G-GFP)*: 4 months,  $n = 5$ ; 6 months,  $n = 6$ ; 7 months,  $n = 6$ ; 8 months,  $n = 4$ ; 12 months,  $n = 19$ ). All blood glucose data are mean  $\pm$  standard deviation. (d) Thirty minutes after intraperitoneal glucose injection, blood was pooled from three to four adult fish and plasma was analyzed by zebrafish C-peptide enzyme-linked immunosorbent assay. Data are mean  $\pm$  standard error of the mean,  $n = 3$  independent experiments.  $P > 0.05$ , one-way analysis of variance with Bonferroni's multiple comparison post-test.

found that mutant hproinsulin failed to undergo anterograde trafficking from the ER, failed to be processed and failed to be secreted. These observations are consistent with *in vitro* studies on this mutant and studies on multiple other insulin mutations that result in misfolded proinsulin<sup>4,13,14,34</sup>. The *in vitro* studies have shown that secretion of co-expressed wild-type insulin is attenuated, and suggest a model in which the cell attempts to compensate by upregulating insulin synthesis. Increased insulin synthesis exacerbates ER stress and might ultimately lead to cell death<sup>33</sup>. Thus, neonatal diabetes caused by mutant insulin is predicted to be associated with severe loss of  $\beta$ -cell mass.

This prediction is supported by diabetic mouse models of misfolded proinsulin, namely the Akita (*Ins2*<sup>WT/C96Y</sup>) mouse<sup>15,27,32,35–37</sup> and Munich (*Ins2*<sup>WT/C95S</sup>) mouse<sup>3</sup>. In both models, the mutant insulin interferes with secretion of wild-type insulin, and  $\beta$ -cell mass is decreased. In the Akita mouse, ER-accumulation of misfolded proinsulin triggers a downstream ER stress response that ultimately results in  $\beta$ -cell apoptosis<sup>27,35</sup>. Although the C96Y mutation (but not C95S) has been reported in human patients with permanent neonatal diabetes, it is unknown whether the pathophysiology is the same in humans and mice<sup>16</sup>.

In our C43G mutant zebrafish model, we found characteristics that parallel some of those found in the mouse models, particularly ER-accumulation of misfolded mutant hproinsulin from as early as 3 dpf. However, the adults were euglycemic, which was not predicted. Although we do not have a definitive explanation for how euglycemia is maintained in these fish, we have several observations suggesting that cell turnover might be

a significant factor. First, adults did not have absolute loss of  $\beta$ -cell mass. Instead,  $\beta$ -cell mass was maintained for at least 12 months. Second, immunostaining showed that the adult  $\beta$ -cell population had a mosaic appearance with respect to GFP accumulation. Although all  $\beta$ -cells expressed GFP, a subpopulation showed massive ER-accumulation whereas another subpopulation within the same islet showed only a modest accumulation, as in larval  $\beta$ -cells. Third, ultrastructure analysis showed that for a subpopulation of  $\beta$ -cells, the ER compartments were indistinguishable from those of the control C-peptide transgenics. Individual cells showed ER stacks with no obvious distention alongside expanded compartments that lacked the electron-dense material seen in adjacent  $\beta$ -cells.

Interestingly, subpopulations of cells have been reported for the Akita mouse, with some cells showing less ER-accumulation of proinsulin than others<sup>1,38</sup>. It has been suggested that these less-affected  $\beta$ -cells represent younger cells that have yet to accumulate significant amounts of misfolded mutant proinsulin in the ER<sup>1</sup>. We hypothesize that for zebrafish, the subpopulation of  $\beta$ -cells with moderate accumulation of GFP is younger than the subpopulation with massive GFP accumulation. In support of this idea, we found that cells with modest GFP accumulation had subcellular localization of endogenous insulin similar to that of larval  $\beta$ -cells. Co-immunostaining for both insulins showed that the mutant form was localized to the ER as predicted, whereas endogenous insulin was localized to cytoplasmic granules. Thus, a pool of endogenous wild-type insulin is available for release by a subpopulation of cells in the mutant islet.

The presence of numerous lacunae and islet architectural rearrangements, along with the ability of the fish to maintain euglycemia, suggest a model in which dysfunctional  $\beta$ -cells are removed and replaced. We hypothesize that  $\beta$ -cells with significantly impacted ER are older, likely have attenuated endogenous insulin secretion and are removed by apoptosis. Younger  $\beta$ -cells, which have endogenous insulin localized to granules, compensate for the impacted cells by secreting sufficient insulin to maintain normal blood sugar. This model is consistent with previous work on  $\beta$ -cell regeneration in zebrafish and its role in maintaining blood glucose homeostasis<sup>30,31</sup>. On-going studies aim to identify the mechanisms of cell removal and replacement (e.g. increased  $\beta$ -cell apoptosis and proliferation) to better understand the regeneration process that is likely occurring in the mutant islet and is responsible for preserving normoglycemia in these fish.

The ability of zebrafish to maintain  $\beta$ -cell mass despite expression of mutant hproinsulin affords a convenient model in which to study the effects of misfolded proinsulin and ER stress in a non-diabetic *in vivo* system. Future proteomic studies might allow us to identify factors critical for maintenance of  $\beta$ -cell mass. This model might also help us to identify pathways of intracellular trafficking as potential therapeutic targets for early-stage diabetic patients.

## ACKNOWLEDGEMENTS

This work was supported by funding from the National Institutes of Health NCRR UL1-RR024999 to the Clinical and Translational Science Awards-Institute for Translational Medicine, P60-DK-20595 to The University of Chicago (UC) Diabetes Research and Training Center, K01-DK-083552 (MDK), K01-DK-075706 (SR), R01-DK-064973 (VEP), R01-DK-48494 (LHP), and JDRF 5-2007-970 (VEP). SCE was supported by a predoctoral fellowship from the Research Training Grant in Digestive Diseases and Nutrition T32-DK07074. The content is solely the responsibility of the authors and does not necessarily represent the official views of the NIDDK or the National Institutes of Health. We thank Christopher Rhodes, Matthew Brady and Graeme Bell for helpful discussions, Michael Parsons (Johns Hopkins) for generously providing the *ins:eGFP/pT2KXIGAIN* plasmid, and, for imaging assistance, Jotham R Austin, II (Electron Microscopy Core Facility, UC), and Vytas Bindokas and Christine Labno (Integrated Microscopy Core Facility, UC). There is no conflict of interest for any of the authors listed.

## REFERENCES

1. Wang J, Takeuchi T, Tanaka S, *et al.* A mutation in the insulin 2 gene induces diabetes with severe pancreatic beta-cell dysfunction in the Mody mouse. *J Clin Invest* 1999; 103: 27–37.
2. Stoy J, Edghill EL, Flanagan SE, *et al.* Insulin gene mutations as a cause of permanent neonatal diabetes. *Proc Natl Acad Sci USA* 2007; 104: 15040–15044.
3. Herbach N, Rathkolb B, Kemter E, *et al.* Dominant-negative effects of a novel mutated Ins2 allele causes early-onset diabetes and severe beta-cell loss in Munich Ins2C95S mutant mice. *Diabetes* 2007; 56: 1268–1276.
4. Colombo C, Porzio O, Liu M, *et al.* Seven mutations in the human insulin gene linked to permanent neonatal/infancy-onset diabetes mellitus. *J Clin Invest* 2008; 118: 2148–2156.
5. Edghill EL, Flanagan SE, Patch AM, *et al.* Insulin mutation screening in 1,044 patients with diabetes: mutations in the INS gene are a common cause of neonatal diabetes but a rare cause of diabetes diagnosed in childhood or adulthood. *Diabetes* 2008; 57: 1034–1042.
6. Molven A, Ringdal M, Nordbo AM, *et al.* Mutations in the insulin gene can cause MODY and autoantibody-negative type 1 diabetes. *Diabetes* 2008; 57: 1131–1135.
7. Polak M, Dechaume A, Cave H, *et al.* Heterozygous missense mutations in the insulin gene are linked to permanent diabetes appearing in the neonatal period or in early infancy: a report from the French ND (Neonatal Diabetes) Study Group. *Diabetes* 2008; 57: 1115–1119.
8. Bonfanti R, Colombo C, Nocerino V, *et al.* Insulin gene mutations as cause of diabetes in children negative for

- five type 1 diabetes autoantibodies. *Diabetes Care* 2009; 32: 123–125.
9. Meur G, Simon A, Harun N, *et al.* Insulin gene mutations resulting in early-onset diabetes: marked differences in clinical presentation, metabolic status, and pathogenic effect through endoplasmic reticulum retention. *Diabetes* 2010; 59: 653–661.
  10. Greeley SA, Naylor RN, Philipson LH, *et al.* Neonatal diabetes: an expanding list of genes allows for improved diagnosis and treatment. *Curr Diab Rep* 2011; 11: 519–532.
  11. Boesgaard TW, Pruhova S, Andersson EA, *et al.* Further evidence that mutations in INS can be a rare cause of Maturity-Onset Diabetes of the Young (MODY). *BMC Med Genet* 2010; 11: 42.
  12. Izumi T, Yokota-Hashimoto H, Zhao S, *et al.* Dominant negative pathogenesis by mutant proinsulin in the Akita diabetic mouse. *Diabetes* 2003; 52: 409–416.
  13. Rajan S, Eames SC, Park SY, *et al.* *In vitro* processing and secretion of mutant insulin proteins that cause permanent neonatal diabetes. *Am J Physiol Endocrinol Metab* 2010; 298: E403–E410.
  14. Park SY, Ye H, Steiner DF, *et al.* Mutant proinsulin proteins associated with neonatal diabetes are retained in the endoplasmic reticulum and not efficiently secreted. *Biochem Biophys Res Commun* 2010; 391: 1449–1454.
  15. Yoshioka M, Kayo T, Ikeda T, *et al.* A novel locus, Mody4, distal to D7Mit189 on chromosome 7 determines early-onset NIDDM in nonobese C57BL/6 (Akita) mutant mice. *Diabetes* 1997; 46: 887–894.
  16. Stoy J, Steiner DF, Park SY, *et al.* Clinical and molecular genetics of neonatal diabetes due to mutations in the insulin gene. *Rev Endocr Metab Disord* 2010; 11: 205–215.
  17. Urasaki A, Morvan G, Kawakami K. Functional dissection of the Tol2 transposable element identified the minimal cis-sequence and a highly repetitive sequence in the subterminal region essential for transposition. *Genetics* 2006; 174: 639–649.
  18. Pisharath H, Rhee JM, Swanson MA, *et al.* Targeted ablation of beta cells in the embryonic zebrafish pancreas using *E. coli* nitroreductase. *Mech Dev* 2007; 124: 218–229.
  19. Kawakami K, Takeda H, Kawakami N, *et al.* A transposon-mediated gene trap approach identifies developmentally regulated genes in zebrafish. *Dev Cell* 2004; 7: 133–144.
  20. Kawakami K. Tol2: a versatile gene transfer vector in vertebrates. *Genome Biol* 2007; 8(Suppl. 1): S7.
  21. Westerfield M. *The Zebrafish Book*. University of Oregon Press, Eugene, 1995.
  22. Huang H, Vogel SS, Liu N, *et al.* Analysis of pancreatic development in living transgenic zebrafish embryos. *Mol Cell Endocrinol* 2001; 177: 117–124.
  23. Pauls S, Geldmacher-Voss B, Campos-Ortega JA. A zebrafish histone variant H2A.F/Z and a transgenic H2A.F/Z:GFP fusion protein for *in vivo* studies of embryonic development. *Dev Genes Evol* 2001; 211: 603–610.
  24. Eames SC, Philipson LH, Prince VE, *et al.* Blood sugar measurement in zebrafish reveals dynamics of glucose homeostasis. *Zebrafish* 2010; 7: 205–213.
  25. Otegui MS, Herder R, Schulze J, *et al.* The proteolytic processing of seed storage proteins in Arabidopsis embryo cells starts in the multivesicular bodies. *Plant Cell* 2006; 18: 2567–2581.
  26. Watkins S, Geng X, Li L, *et al.* Imaging secretory vesicles by fluorescent protein insertion in propeptide rather than mature secreted peptide. *Traffic* 2002; 3: 461–471.
  27. Liu M, Hodish I, Rhodes CJ, *et al.* Proinsulin maturation, misfolding, and proteotoxicity. *Proc Natl Acad Sci USA* 2007; 104: 15841–15846.
  28. Rubenstein AH, Clark JL, Melani F, *et al.* Secretion of proinsulin C-peptide by pancreatic  $\beta$ -cells and its circulation in blood. *Nature* 1969; 224: 697–699.
  29. Stadelmann C, Lassmann H. Detection of apoptosis in tissue sections. *Cell Tissue Res* 2000; 301: 19–31.
  30. Curado S, Anderson RM, Jungblut B, *et al.* Conditional targeted cell ablation in zebrafish: a new tool for regeneration studies. *Dev Dyn* 2007; 236: 1025–1035.
  31. Moss JB, Koustubhan P, Greenman M, *et al.* Regeneration of the pancreas in adult zebrafish. *Diabetes* 2009; 58: 1844–1851.
  32. Oyadomari S, Koizumi A, Takeda K, *et al.* Targeted disruption of the Chop gene delays endoplasmic reticulum stress-mediated diabetes. *J Clin Invest* 2002; 109: 525–532.
  33. Liu M, Hodish I, Haataja L, *et al.* Proinsulin misfolding and diabetes: mutant INS gene-induced diabetes of youth. *Trends Endocrinol Metab* 2010; 21: 652–659.
  34. Liu M, Haataja L, Wright J, *et al.* Mutant INS-gene induced diabetes of youth: proinsulin cysteine residues impose dominant-negative inhibition on wild-type proinsulin transport. *PLoS ONE* 2010; 5: e13333.
  35. Hodish I, Liu M, Rajpal G, *et al.* Misfolded proinsulin affects bystander proinsulin in neonatal diabetes. *J Biol Chem* 2010; 285: 685–694.
  36. Kayo T, Koizumi A. Mapping of murine diabetogenic gene mody on chromosome 7 at D7Mit258 and its involvement in pancreatic islet and beta cell development during the perinatal period. *J Clin Invest* 1998; 101: 2112–2118.
  37. Ron D. Proteotoxicity in the endoplasmic reticulum: lessons from the Akita diabetic mouse. *J Clin Invest* 2002; 109: 443–445.
  38. Hodish I, Absood A, Liu L, *et al.* *In vivo* misfolding of proinsulin below the threshold of frank diabetes. *Diabetes* 2011; 60: 2092–2101.